Transcallosal generation of phase aligned beta-bursts underlies TMS-induced interhemispheric inhibition

Christian Georgiev[1,*], Scott J. Mongold[1], Pierre Cabaraux[2], Gilles Naeije[2,3,4], Julie Duque[5], Mathieu Bourguignon[1,3,6]

1. Laboratory of Functional Anatomy, Faculty of Human Motor Sciences, Université libre de Bruxelles (ULB), Brussels, Belgium
2. Department of Neurology, Hôpital universitaire de Bruxelles (HUB), Université libre de Bruxelles (ULB), Brussels, Belgium
3. Laboratoire de Neuroanatomie et Neuroimagerie translationnelles, UNI – ULB Neuroscience Institute, Université libre de Bruxelles (ULB), Brussels, Belgium.
4. Centre de Référence Neuromusculaire, Department of Neurology, CUB Hôpital Erasme, Université libre de Bruxelles (ULB), Brussels, Belgium.
5. Institute of Neuroscience, Université catholique de Louvain, Brussels, Belgium.
6. WEL Research Institute, avenue Pasteur, 6, 1300 Wavre, Belgique.

* Correspondence to Christian.Georgiev@ulb.be; Université Libre de Bruxelles, Route de Lennik 808, B-1070 Brussels, Belgium.

Conflicts of interest statement: The authors have no conflicts of interest to declare.

Abstract

Background

The excitability of the sensorimotor (SM1) cortices is reflected in the bilateral ~20 Hz beta oscillations. The extent to which these oscillations subtend the interhemispheric inhibition captured by the Transcranial Magnetic Stimulation (TMS) ipsilateral Silent Period (iSP) protocol is unknown.

Objectives

We investigated the relationship between movement-induced beta suppression, iSP, and manual dexterity.

Methods

Forty adults underwent an Electroencephalography assessment of beta oscillations during volitional left hand movement and a TMS assessment of iSP recorded from the right hand**.** In both cases, left SM1 beta oscillations (contralateral to the activated right SM1), were monitored through a proxy signal – the Electromyography of the contracted right hand. Manual dexterity was assessed with the Purdue Pegboard Test.

Results

Volitional movement caused significant bilateral SM1 beta suppression in nearly all participants (≥ 85 %). ISPs were observed in every participant. In the proxy signal for the left SM1, the iSP coincides with TMS-induced high-amplitude beta bursts. These bursts showed significant phase alignment across participants 10–70 ms after the TMS pulse. There was no significant association between the left-/right-hemisphere beta suppression, iSP, and manual dexterity.

Conclusion

Our results highlight the distinct nature of beta oscillation changes during voluntary movement compared to TMS-iSP and show that TMS induces IHI via transcallosal induction of phase aligned beta bursts. Furthermore, our data suggests that only the initial phase of a beta burst carries an inhibitory effect. It also highlights the possibility of evoking a beta burst with the iSP protocol, opening perspectives for future modeling studies.

Keywords: Beta oscillation, Beta bursts, Phase-alignment, Interhemispheric inhibition, Ipsilateral silent period, Motor dexterity

Highlights

- Movement-induced beta suppression does not reflect Transcranial Magnetic Stimulation-induced interhemispheric inhibition
- Transcranial Magnetic Stimulation induces interhemispheric inhibition via transcallosal induction of phase aligned high-amplitude beta bursts
- The inhibitory effect of a beta burst appears to be carried by its initial oscillatory cycle
- Beta oscillations and interhemispheric inhibition's role for motor dexterity need further exploration

1. Introduction

Beta oscillations are commonly observed in Electroencephalography (EEG) and Magnetoencephalography (MEG) recordings of the primary sensorimotor cortex (SM1) [1–5]. They are comprised of non-rhythmic ~100 ms 13-30 Hz bursts [6–8] that are suppressed shortly before and during bodily movement and enhanced after movement [9–12]. Numerous studies have implicated beta oscillations in the balancing of excitatory and inhibitory processes within the SM1 [13,14]. Particularly, a suppression of beta bursts reflects the emerging neuronal activation within a given somatotopic region necessary for movement initiation. Conversely, enhanced beta burst amplitude and rate reflect the subsequent incoming wave of neuronal inhibition necessary for discontinuing any unwanted residual movement [15,16]. Based on such findings, the magnitude of beta suppression is a frequently used index for investigating activation within the SM1s [9–11].

The ability of beta oscillations to sustain themselves and synchronize distant cortical areas [17] has led researchers to investigate beta dynamics on a larger scale. This has provided consistent evidence that the SM1 beta suppression becomes bilateral after movement execution [4,18,19]. Such bilaterality defines a sensorimotor beta-band network, the operations of which have been associated with motor learning [20,21] and motor performance [22,23]. However, the extent to which such large-scale bilateral beta oscillatory dynamics reflect the transcallosal regulation of excitation and inhibition of the two SM1s remains mostly unclear.

Complex dynamics of interhemispheric signaling, through which the SM1s regulate each other's excitability, underlie dexterous unimanual and bimanual motor performance [24]. The mechanism theorized to produce these bilateral SM1 interactions is

Interhemispheric Inhibition (IHI) [25–31]. IHI is a process through which activation of one brain region selectively suppresses activation of its homologous region in the contralateral hemisphere [32]. IHI has been widely investigated with Transcranial Magnetic Stimulation (TMS) paradigms, among which is the ipsilateral Silent Period (iSP). The iSP manifests as a suppression of the Electromyography (EMG) activity of a contracted muscle ~50 ms after a TMS pulse is applied above the ipsilateral primary motor cortex (M1) representation of that muscle [25,28,30,33–36]. The TMS pulse transcallosally inhibits the contralateral SM1 which disrupts its efferent output and results in the silenced contralateral (ipsilateral to the TMS pulse) EMG [37]. Considering the strong implication of beta oscillations in cortical inhibition raises the question of whether the changes in M1 excitability underpinning TMS-induced iSP originate in left-/right-hemisphere modulations of beta oscillations.

Previous research with simultaneous TMS-EEG has shown that the induction of IHI is contingent on the excitability of both the stimulated and the inhibited SM1 [38,39] and the potency of a TMS pulse is contingent on the amplitude, rate, and phase of naturally occurring beta bursts [40,41]. However, the amplitude of beta oscillations and of their movement-induced modulation is highly variable across individuals [42], prompting the question whether this inter-individual variability reflects differences in IHI captured by the iSP. Furthermore, it is unclear which feature (amplitude or phase) of the beta bursts carries the inhibitory effect. Interestingly, single-pulse TMS above a certain brain region can alter the phase of neuronal oscillations both within that given region [43,44] as well as in another anatomically connected brain region [45–47]. Therefore, it could be hypothesized that an iSP-inducing TMS pulse alters contralateral beta oscillations in a

manner akin to the phase resetting theorized to underlie neural information transfer [48,49].

To elucidate the extent to which beta amplitude and phase alterations reflect IHI processes, we conducted an experiment with non-simultaneous EEG, TMS, and motor dexterity assessments. We investigated the extent to which bilateral changes in beta amplitude during volitional movement are predictive of iSP strength. Subsequently, in line with how the iSP is interpreted as a proxy for inhibition at the level of the SM1s, we used the EMG of the contracted muscle during the iSP protocol as a proxy for assessing the effect of the TMS pulse on the contralateral cortical beta oscillations [50–53]. We hypothesized that the occurrence of an iSP coincides with a TMS-induced contralateral enhancement of beta amplitude, attributable to the generation of phase aligned beta bursts. Lastly, to explore the behavioral relevance of the beta oscillations and the iSP, we investigated their association with bimanual motor dexterity.

2. Methods

Forty (16 female; Mean ± SD age = 24.5 ± 4.4, range 20-49 years) adult volunteers with normal or corrected-to-normal vision and hearing participated in the study. All participants were right-handed [54], did not suffer from neurological or psychiatric disorders, did not take any medication known to alter cerebrocortical excitability, and had no contraindications to TMS. The experimental protocol was approved by the ethics committee of the CUB Hôpital Erasme (CCB, B4062023000234) and the experiment was conducted in accordance with the Declaration of Helsinki. All participants signed an informed consent prior to participation.

2.1 Experimental Protocol

The protocol was divided into three parts: an EEG assessment of cortical beta oscillations, a TMS assessment of IHI, and a behavioral assessment of bimanual dexterity. The three parts of the experiment were conducted in a randomized order within a single session.

EEG assessment of the cortical beta oscillations. Participants maintained a stable isometric pinch-grip contraction with the right thumb and index finger against a force transducer (RS Pro, P/N 1004-0.6 kg) at 10 ± 3 % of their maximum voluntary contraction (MVC) force. MVC was individually determined for each participant prior to the start of the experiment. Task compliance was ensured with visual feedback prompting participants to increase their force when it subceeded 7 % MVC and to decrease their force when it exceeded 13 % MVC. While engaged in the isometric contraction with the right hand, once

every 3–4 s (random jitter), participants were presented with an auditory tone prompting them to perform a fast closing/opening motion with the fingers of their non-contracted left hand (Figure 1A). This task was performed for 2 blocks of 5 minutes with a short break in between.

Throughout the task, 64 Ag/AgCl-sintered electrode EEG (EEGO Mylab, ANT Neuro, Hengelo, the Netherlands) was recorded. Electrode impedance was kept blow 20 kΩ. The recording was online referenced to electrode CPz, and sampled at 1 kHz. The signals of a 3-axis accelerometer (ADXL335, AnalogDevices, Wilmington, MA, USA) attached to the index finger of the closing/opening left hand were recorded in synchrony with the EEG signals.

Surface EMG (COMETA Pico, COMETA, Milan, Italy) from the contracted right First Dorsal Interosseous (FDI) muscle was recorded with a sampling frequency of 1 kHz. EMG was recorded in a monopolar configuration, with an “active” electrode placed above the muscle belly, and a “reference” electrode placed above the first metacarpal bone. The EEG and EMG acquisitions were synchronized via the delivery of triggers.

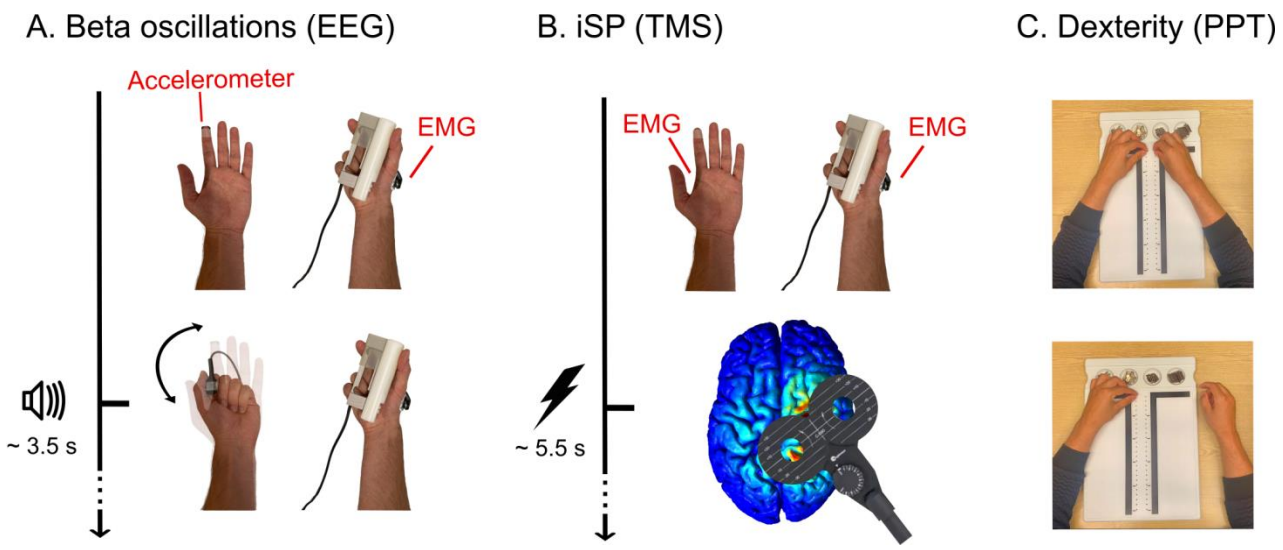

Figure 1. Experimental protocol. For assessing EEG beta oscillations, participants held a constant contraction with their right hand, and performed left hand movements in response to auditory prompts (A). For assessing IHI, participants underwent an iSP protocol with a constant contraction with their right hand and single-pulse TMS applied above the ipsilateral M1 (B). For assessing manual dexterity, participants performed the PPT (C).

TMS assessment of the iSP. Participants were seated on a chair equipped with a neck brace for securing the head into position and minimizing unwanted movements. Surface EMG from the left and right FDI muscles were recorded as in the EEG task.

The hotspot corresponding to the hand area on the right M1 was identified via biphasic single-pulse TMS (MagPro X100, MagVenture, Farum, Denmark) with a hand-held figure-of-eight coil (7.5 cm external loop diameter), pointed 45° away from the midline. Each participant's Resting Motor Threshold (RMT) was identified following the standard procedure [55].

During the iSP task, participants held an isometric contraction with their right hand as done in the EEG task, while completely relaxing their left hand. Once every 5–6 s (random jitter) a TMS pulse was delivered to the previously identified hotspot with an intensity of 130 % RMT (Figure 1B). The procedure was performed for 2 blocks of 4.5 minutes, resulting in a total of 100 iSPs per participant.

Behavioral assessment of unimanual dexterity and bimanual coordination.

Participants completed the Purdue Pegboard Test (PPT; [56]). The PPT assesses the fine motor performance of the left hand (PPT_{LH}), right hand (PPT_{RH}), both hands in synchrony (PPT_{BH}), and both hands in alternation ($PPT_{assembly}$; *Figure 1C*). Scores were computed following the PPT guidelines. Two additional bimanual coordination scores were computed. The first coordination score (PPT_{C1}) was the $PPT_{Assembly}$ divided by the geometric mean of the PPT_{LH} and PPT_{RH}. The second PPT coordination index (PPT_{C2}) was the $PPT_{Assembly}$ divided by the PPT_{BH}.

2.2 EEG and EMG Data Processing

EEG preprocessing. EEG data was preprocessed offline with a custom MATLAB (Mathworks, Natick, MA) script and the FieldTrip toolbox [57]. Bad channels were identified (following the guidelines of [58]) and topographically interpolated. EEG signals were re-referenced to a common average, filtered through 0.3–45 Hz, and Independent Components Analysis [59] was used for further artifact suppression. Twenty independent components were evaluated from the data and, on average, 4 (SD = 1.3) independent components per participant were removed.

Beta amplitude modulation analysis. EEG signals were filtered through 5-Hz-wide frequency bands centered on 5–40 Hz by steps of 1 Hz as done in [52,53]. EEG signals were smoothly set to 0 (squared-cosine transition of 1 s) at timings 1 s around artifacts (timepoints where full-band EEG amplitude in at least one electrode exceeded 5 SDs above the mean), and to avoid edge effects, further analyses were based on timepoints at least 2 s away from artifacts and appearance of force visual feedback. Subband signals' envelope was then extracted with the Hilbert transform. To avoid contamination by very slow envelope variations, these subband envelopes were divided by their low-pass filtered version at 0.1 Hz [52,53]. As a further normalization, the envelopes were centered on 0 by subtracting the value 1, and converted to percentage of change by multiplying by 100 %.

Subband envelopes were segmented into epochs from –1000 to 2500 ms relative to left hand movement onset as identified in accelerometer recordings. Epochs which contained time points less than 2 s away from artifacts or in which participants failed to perform a movement or failed to maintain the force in the desired range were excluded from the analysis. The remaining epochs (113 ± 25, Mean ± SD across participants) were subsequently averaged across trials, giving rise to a time-frequency map of amplitude modulation for each EEG channel and each participant. Further analyses were focused on preselected electrodes spanning the left (C1, C3, C5, CP1, CP3, CP5, FC1, FC3, FC5) and right (C2, C4, C6, CP2, CP4, CP6, FC2, FC4, FC6) SM1s. We further retained the electrode above each SM1 which showed the maximal amplitude suppression in a preselected time-frequency window ranging from –500 to 1000 ms relative to left hand

movement onset and from 13 to 30 Hz. Left and right SM1 EEG beta suppressions were quantified using the size of the cluster of significant beta suppression (β_{size}; see subsection statistical analyses) and the minimal value within the above defined time-frequency window (β_{depth}). Lastly, to highlight left-/right-hemisphere imbalance in beta modulations, contrasts between the left and right indices of beta suppression were computed as their difference (left minus right) divided by their sum, leading to $\Delta\beta_{size}$ and $\Delta\beta_{depth}$.

EMG iSP preprocessing and analysis. The EMG data from the contracted rFDI during the iSP protocol was preprocessed offline with a custom MATLAB script. Data were filtered between 20 and 295 Hz, followed by notch filters at 50 Hz and its harmonics, and rectified. The EMG was segmented into epochs from –100 to 200 ms relative to TMS pulse onset. The epochs were averaged within participants and normalized by their baseline mean (taken from 50 ms to 5 ms prior to the TMS pulse), and used for iSP quantification. The iSP onset and offset were identified with Mean Consecutive Difference thresholding [60,61] and used for computing iSP latency (time between the TMS pulse and the iSP onset), iSP duration (time between the iSP onset and offset), and normalized iSP area (integral of the normalized rectified EMG signal between the iSP onset and offset [60]).

Time-frequency and phase domain EMG analyses. To further characterize the beta modulations induced by the voluntary movements and the TMS-iSP protocol, we used the unrectified FDI EMG of the contracted right hand during each task as a proxy for the changes occurring in the contralateral SM1 [50–53]. EMG signals were filtered in

subbands for envelope extraction, segmented, and averaged as previously done with the EEG signals.

We further analyzed the unrectified right FDI EMG to determine whether TMS-induced iSP relates to a phase resetting of contralateral beta oscillations. Thus, the unrectified EMG was filtered between 13 and 30 Hz and segmented into epochs from –200 to 500 ms relative to TMS pulse onset. Epochs were normalized by their root-mean-square amplitude in the interval –50 to –5 ms and averaged across trials. Hilbert transformation was applied to the averaged EMG trace of each participant. Then, we determined whether Hilbert coefficients at time points from 0 to 200 ms by step of 10 ms tended to show a consistent phase. Due to the uncertainty regarding EMG polarity (which is dependent on the choice of the active and reference electrodes that was not standardized across participants), phase consistency was assessed using an approach based on singular value decomposition (SVD). More precisely, for each time-point, SVD was applied to all participants' Hilbert coefficients arranged as a matrix with the real part of all participants' coefficients stacked as the first column and the imaginary part as the second column. The first singular value of the decomposition was used to quantify the strength of the phase alignment across participants.

2.3 Statistical analyses.

Movement-induced EEG and EMG beta suppression. Non-parametric cluster-based tests were applied to each participant's EEG data to assess the significance of β_{size} in relation to left hand movements, separately for the left (ipsilateral) and right (contralateral) hemisphere electrodes. In brief, 10000 surrogate amplitude modulation

maps were built based on EEG subband envelopes segmented with respect to random onsets separated by 3–4 s. These surrogate maps served to identify β_{size}, for the genuine and each surrogate data, which was the size of the largest cluster of time-frequency bins displaying a larger amplitude suppression or enhancement than their percentile 95 across all maps. The *p*-value for β_{size} was obtained as the proportion of surrogate β_{size} values that were higher than the observed genuine value.

Analogous non-parametric tests were applied to the time-frequency maps of EMG amplitude.

TMS-induced EMG beta phase reset. Surrogate-data-based statistics were applied to evaluate the significance of the TMS-induced phase alignment in the beta band of the right FDI EMG. To do so, the strength of the phase alignment across participants for each time point after the TMS pulse was compared to a null distribution obtained using the Hilbert coefficients with a phase randomly selected in the range [-π, π] (10000 repetitions) while preserving the amplitude. The *p*-value was obtained as the proportion of values in the null distribution that were higher than the genuine singular value.

Association Analyses. Redundancy analysis (RDA) was used to investigate the relationships between all constructs of interest. RDA is a multivariate technique for modeling the effect of a linear combination of a set of related predictors on the linear combinations of a set of related outcomes [62]. In two RDA models, we assessed i) the predictive power of all indices of beta suppression on all indices of iSP and ii) the predictive power of all indices of beta suppression and iSP together on all indices of bimanual motor dexterity. Statistical significance of each model was assessed with RDA Monte Carlo permutation tests with 10000 permutations.

3. Results

3.1 Movement-induced beta suppression.

The EEG analyses identified a large-scale suppression of the beta amplitude following hand movement (Figure 2). More quantitatively, in the time interval from –500 to 1000 ms, β_{size}, was significant in 35 (87.5 %) participants ($p < 0.05$) in the contralateral (right) hemisphere, and in 34 (85 %) participants ($p < 0.05$) in the ipsilateral (left) hemisphere. Across participants, the contralateral β_{size} was 100.5 ± 85.9 and the ipsilateral β_{size} was 84.4 ± 73.3 time-frequency bins, while the contralateral β_{depth} was 26.1 ± 6.2 % and the ipsilateral β_{depth} was 24.1 ± 4.8 %. Contralateral β_{size} and β_{depth} were significantly larger than their ipsilateral counterparts (β_{size}, $t_{39} = 2.4$, $p = 0.024$; β_{depth}, $t_{39} = 4.4$, $p < 0.0001$).

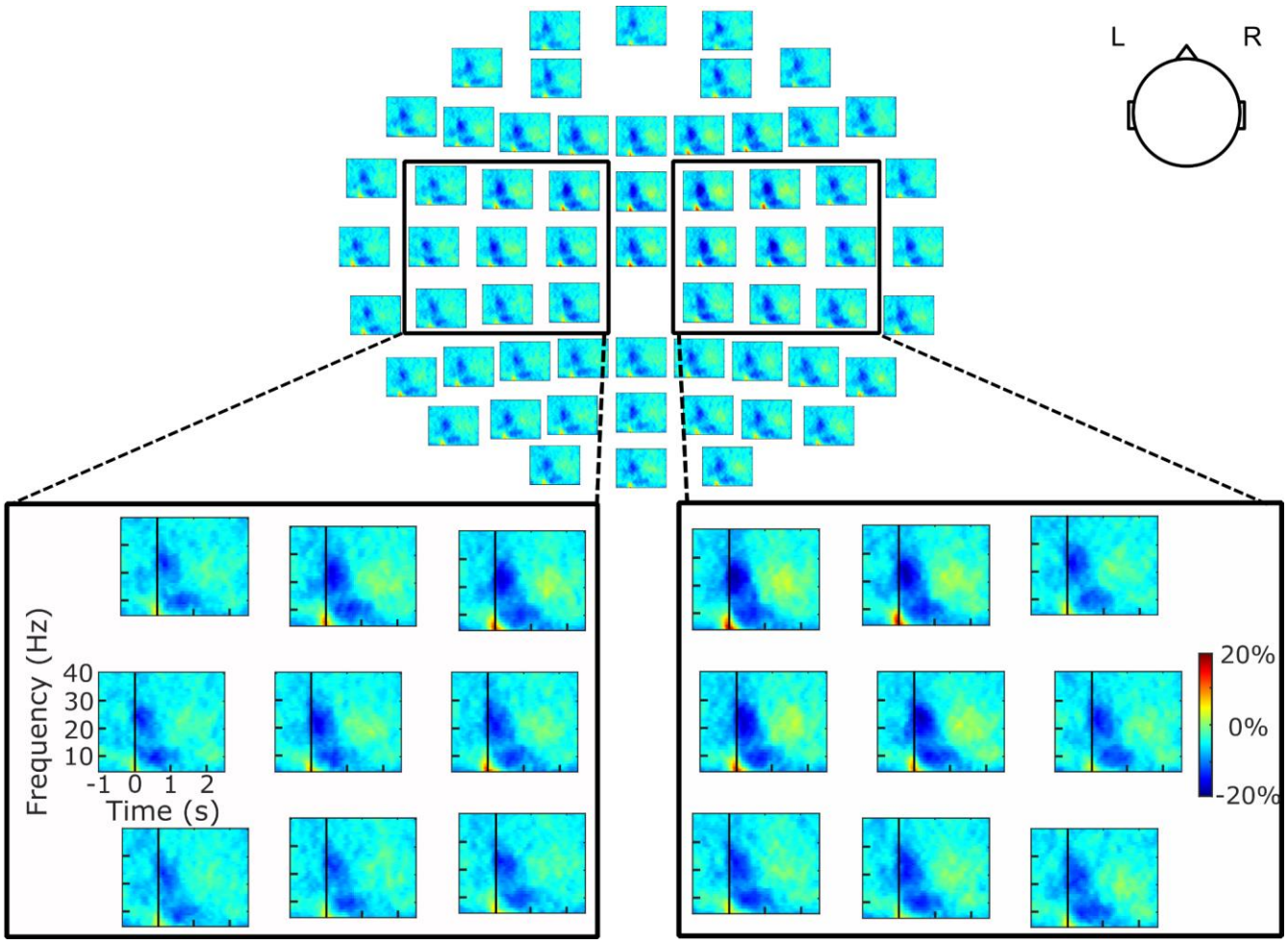

Figure 2. Group-averaged scalp distribution of the time-frequency maps of amplitude modulation during the volitional movement task. The black rectangles outline the data for the 9 electrodes of interest above each hemisphere's SM1 and the black vertical lines at time 0 indicate the onset of left hand movement.

3.2 TMS-induced iSP.

The RMT of our sample was 50.0 ± 8.6 % of the maximal stimulation intensity of the TMS device.

An iSP was identified in all participants (Figure 3), in the form of decreased muscle activity ~50 ms after TMS stimulation, characterized by a latency of 39.3 ± 6.2 ms, a duration of 25.1 ± 7.6 ms, and a normalized area of 7.1 ± 3.5 mV ms. Of note, iSPs were shortly followed by two successive peaks of increased muscle activity up until ~150 ms.

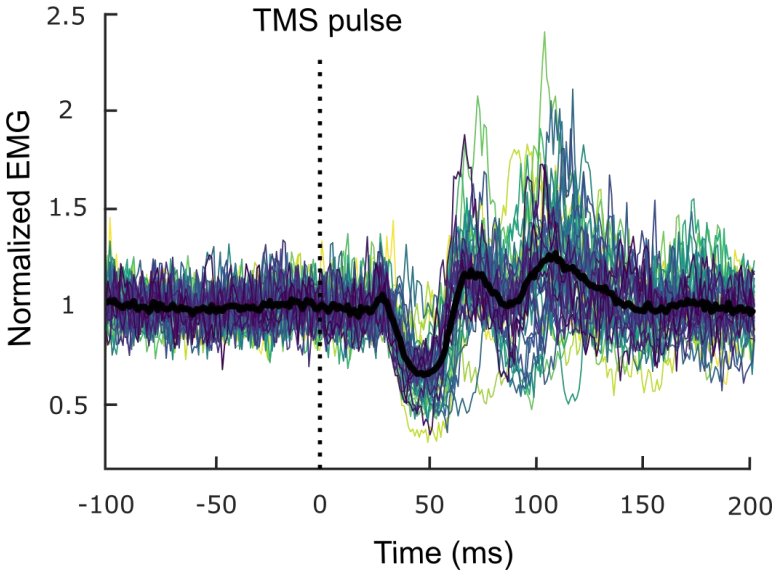

Figure 3. Normalized rectified EMG traces (averaged across trials) during the iSP task. There is one trace per participant and the black trace corresponds to their grand average. The vertical dotted black line indicates the TMS pulse onset.

3.3 Time-frequency domain EMG changes.

Figure 4A presents the group-averaged time-frequency map of the amplitude of the rFDI EMG signal in the volitional movement task. It highlights a large-scale suppression of

the beta amplitude corresponding to the onset of the left hand movement, reflecting that observed in the left SM1 (Figure 2). In the time interval from –500 to 1000 ms, EMG β_{size} was 53.2 ± 60.9 time-frequency bins and was statistically significant in 29 (72.5 %) participants ($p < 0.05$).

Figure 4B presents the group-averaged time-frequency map of the amplitude of the rFDI EMG signal in the iSP task. Contrasting with Figure 4A, it shows a large-scale enhancement of spectral amplitude at frequencies up to 30 Hz after TMS pulse, along with a discernible maximum at beta frequencies localized between 50 and 200 ms. In the time interval from –500 to 1000 ms, EMG β_{size} was 42.1 ± 31.0 time-frequency bins and was statistically significant in 32 (80 %) participants ($p < 0.05$).

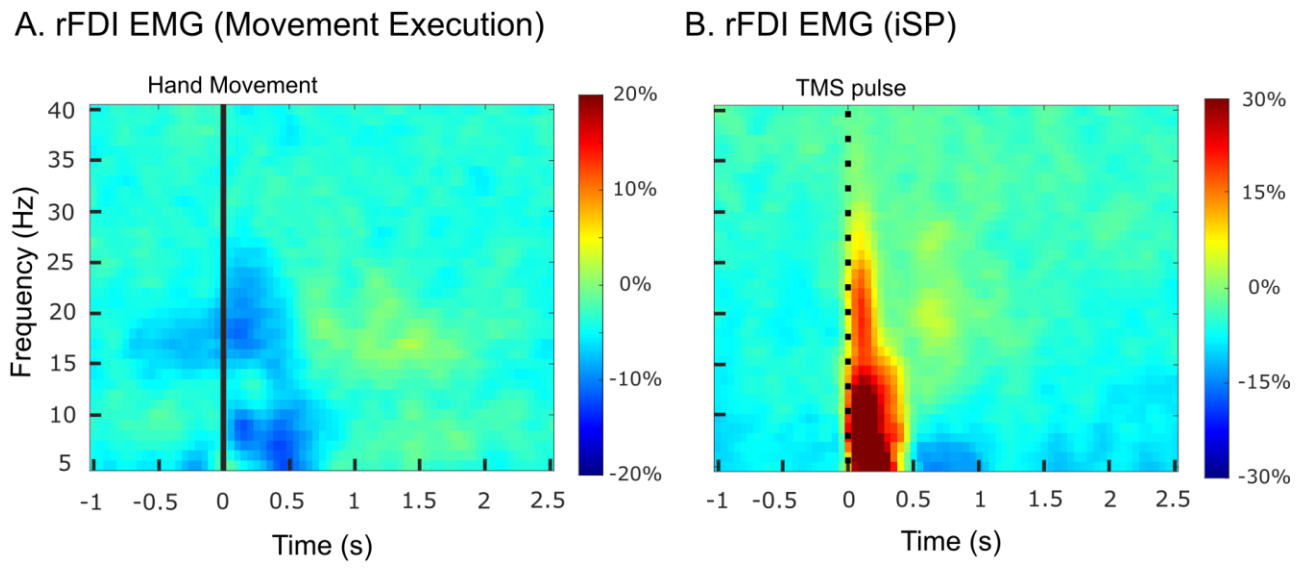

Figure 4. Group-averaged time-frequency map of the right FDI EMG amplitude during the volitional movement task (A) and the iSP task (B).

3.4 Phase domain EMG changes.

Figure 5 presents the time-course of the averaged normalized non-rectified EMG traces filtered through 13–30 Hz in the TMS-iSP protocol. It highlights the presence of a beta oscillation starting from 20–30 ms after the TMS pulse. Importantly, the first peak of this oscillation appeared consistently at 40 ms across participants. And indeed, the phase consistency analysis revealed a significant phase alignment of Hilbert coefficients in the time interval 10 to 70 ms following the onset of the TMS pulse ($p < 0.05$), with the beta phase alignment reaching maximal significance at 40 ms after the TMS pulse ($p = 0.0003$; Figure 5). This demonstrates that 10 to 70 ms after the TMS pulse, ipsilateral EMG beta oscillations align in phase and then diverge over time, possibly due to interindividual variability in the shape of the beta bursts.

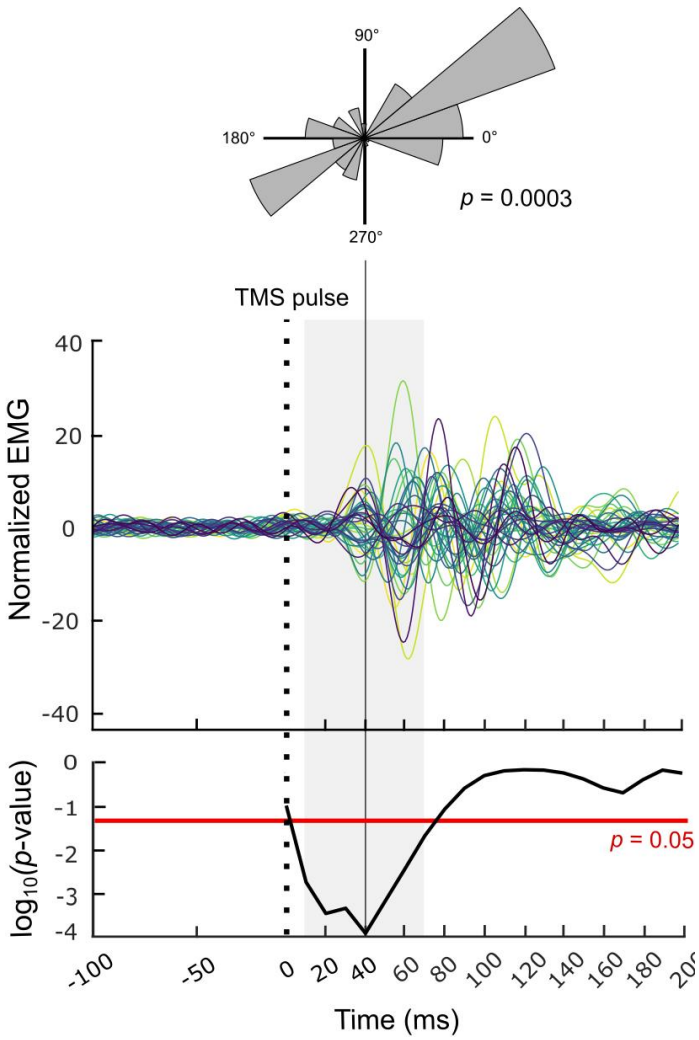

Figure 5. Normalized non-rectified EMG traces (averaged across trials) of each participant in the iSP task demonstrating the signals' phase alignment, along with its corresponding p-value. The vertical dotted black line indicates the TMS pulse; the horizontal red line indicates the threshold for statistical significance and the shaded gray area indicates the time period of significant phase alignment. The top inset presents the phase distribution of the Hilbert coefficients across participants. For each angle interval (20 in total, covering 0 to 360°), it presents the sum of Hilbert coefficients' amplitude whose phase lies in this interval.

3.6 Association analyses.

The RDA aimed at assessing the relationships between the indices of left-/right-hemisphere beta imbalance ($\Delta\beta_{size}$ and $\Delta\beta_{depth}$), iSP (latency, duration, and normalized area), and bimanual motor performance (PPT_{BH}, $PPT_{Assembly}$, PPT_{C1}, and PPT_{C2}) revealed that, collectively, the beta modulation indices did not explain a significant proportion of variance of the iSP indices (4.4 %, $F_{2,37} = 0.85$, $p = 0.48$). It also revealed that, collectively, the beta modulation and iSP indices did not explain a significant proportion of variance of bimanual dexterity (12.7 %, $F_{5,34} = 0.99$, $p = 0.44$). Participants' PPT scores and the results of univariate correlations between all variables are presented in Supplementary Results 1.

4. Discussion

Our study aimed at elucidating the link between the changes of SM1 beta oscillations and IHI processes and investigating the behavioral relevance of the two phenomena. We did not find a significant association between the inter-individual variability in the left-/right-hemisphere imbalance in SM1 beta suppression during volitional movement, iSP, and motor dexterity. However, we found that TMS-iSP is contingent on the rapid induction of a phase-aligned beta burst in the hemisphere contralateral to the stimulation, a process opposite in nature to the ipsilateral beta suppression observed during voluntary movement.

4.1 Contrasting modulation of contralateral SM1 beta oscillations by voluntary movement and TMS

Using the FDI EMG of the contracted right hand as a proxy for the changes occurring in the contralateral SM1 [50–53], we demonstrated a striking divergence in beta SM1 oscillatory dynamics during volitional movement and during TMS-induced iSP. Indeed, ipsilateral SM1 beta activity was suppressed following a hand movement, consistent with an extensive literature [1,4,19], while delivering a TMS pulse to SM1 resulted in a significant enhancement of contralateral beta amplitude, attributable to the generation of beta bursts. In addition, more pronounced ipsilateral beta rhythm amplitude suppression (relative to contralateral) was not associated with classical iSP parameters. Therefore, the ubiquitous beta rhythm suppression in the hemisphere ipsilateral to hand movement appears to receive minimal contribution from the IHI regulatory processes captured by the iSP. Even if naturally occurring IHI processes during voluntary movement would encompass a contralateral beta burst induction of the type highlighted in our iSP results, the presence of such a hypothetical burst would be obscured by the co-occurring large-scale beta suppression. In any case, the absence of association between measures of movement-induced beta modulation and TMS-induced iSP suggests that these two phenomena reflect two distinct types of interhemispheric interactions occurring at different time scales.

The distinct nature of the beta rhythm changes during movement compared to TMS-IHI can be explained by the vastly distinct state of the motor system during each task [44]. The suppression in the beta rhythm during voluntary movements results from goal-directed action planning, followed by motor command formulation, initiation, and constant

refinement, as orchestrated by a distributed prefrontal [63], premotor [64], SM1, and Parietal [65] system. On the other hand, the IHI processes captured by iSP are manifestations of a very rapid strong excitation of a SM1 hotspot in the absence of any volition to move. Such excitation does not have the crucial role of precisely executing a desired movement and therefore engages the distributed sensorimotor system in a distinct way. Therefore, in the case of TMS-iSP, the TMS-induced beta burst in the contralateral hemisphere causes a fleeting inhibitory process which interacts with the natural brain oscillations, yet lacks the functional relevance of the amplitude modulations of the beta rhythm during movement. Overall, these considerations suggest that the importance of TMS-induced IHI for motor control might have been overestimated, as it may represent a trifling mechanism that is completely overshadowed by the surrounding brain activity.

4.2 TMS-induced phase resetting of contralateral SM1 beta oscillations

We found that the beta enhancement observed in the proxy signal for the SM1 contralateral to that stimulated with TMS coincides with a consistent phase alignment of beta oscillations. This alignment was most evident ~40 ms after the TMS pulse in the proxy signal, but would likely occur ~20 ms after TMS in SM1 given the well-documented ~20-ms propagation delay from SM1 to EMG [66]. The beta phase alignment indicates that a phase-resetting mechanism underlies the iSP. Phase resetting effects of TMS have previously been reported for naturally occurring theta, alpha, and beta oscillatory activity within the stimulated SM1 [43,45], but not in the contralateral SM1 and not in relation to IHI. Expanding upon the perspective whereby beta oscillations consist of short-lived bursts [6–8,67], which have an inhibitory effect on the motor system, our data suggests that it is

the phase of the initial peak of the burst that carries the inhibitory effect. This is evidenced by the near-exact co-occurance of the initial peak of the beta bursts (Figure 5) and the onset of the iSP (Figure 3) at ~40 ms after the TMS pulse. Therefore, the TMS-iSP protocol, able to generate contralateral beta bursts, could serve future investigations of the nature of the beta oscillations by comparing the properties of the TMS-generated burst to the predictions of computational models of neural oscillations [68].

4.3 Limitations and perspectives

Since we assessed beta oscillations, iSP, and manual dexterity non-simultaneously, we could only capitalize on inter-individual variability to identify brain-behavioral relationships. However, previous research has found behavioral relevance of beta modulation and iSP predominantly with in-task assessments of motor performance [69–73] while investigations quantifying motor performance with motor dexterity tests paint a less clear picture [74]. Future studies should clarify the task-specificity of the behavioral relevance of beta oscillations and IHI. If beta oscillations and IHI truly are the crucial motor system regulatory mechanisms they are theorized to be [32,75], their role for motor behavior should likely extend beyond in-task effects.

4.4 Conclusion

Our study clarified the beta oscillatory dynamics underlying TMS iSP. It underlies crucial differences with naturally occurring beta dynamics, suggesting that phenomena observed in TMS-IHI studies may not generalize to natural motor control. However, the

TMS iSP protocol offers a means to observe and analyze beta bursts, as well as to support computational modeling studies.

References

1. Démas J, Bourguignon M, Périvier M, De Tiège X, Dinomais M, Van Bogaert P. Mu rhythm: State of the art with special focus on cerebral palsy. Ann Phys Rehabil Med. 2020;63: 439–446.

2. Pfurtscheller G. Central beta rhythm during sensorimotor activities in man. Electroencephalogr Clin Neurophysiol. 1981;51: 253–264.

3. Salenius S, Hari R. Synchronous cortical oscillatory activity during motor action. Curr Opin Neurobiol. 2003;13: 678–684.

4. Pfurtscheller G, Lopes da Silva FH. Event-related EEG/MEG synchronization and desynchronization: basic principles. Clin Neurophysiol. 1999;110: 1842–1857.

5. Neuper C, Wörtz M, Pfurtscheller G. ERD/ERS patterns reflecting sensorimotor activation and deactivation. Prog Brain Res. 2006;159: 211–222.

6. Shin H, Law R, Tsutsui S, Moore CI, Jones SR. The rate of transient beta frequency events predicts behavior across tasks and species. Elife. 2017;6. doi:10.7554/eLife.29086

7. Szul MJ, Papadopoulos S, Alavizadeh S, Daligaut S, Schwartz D, Mattout J, et al. Diverse beta burst waveform motifs characterize movement-related cortical dynamics. Prog Neurobiol. 2023;228: 102490.

8. Enz N, Ruddy KL, Rueda-Delgado LM, Whelan R. Volume of β-bursts, but not their rate, predicts successful response inhibition. J Neurosci. 2021;41: 5069–5079.

9. Kilavik BE, Zaepffel M, Brovelli A, MacKay WA, Riehle A. The ups and downs of β oscillations in sensorimotor cortex. Exp Neurol. 2013;245: 15–26.

10. Diesburg DA, Greenlee JD, Wessel JR. Cortico-subcortical β burst dynamics underlying movement cancellation in humans. Elife. 2021;10. doi:10.7554/eLife.70270

11. Little S, Bonaiuto J, Barnes G, Bestmann S. Human motor cortical beta bursts relate to movement planning and response errors. PLoS Biol. 2019;17: e3000479.

12. Wagner J, Makeig S, Gola M, Neuper C, Müller-Putz G. Distinct β Band Oscillatory Networks Subserving Motor and Cognitive Control during Gait Adaptation. J Neurosci. 2016;36: 2212–2226.

13. Sherman MA, Lee S, Law R, Haegens S, Thorn CA, Hämäläinen MS, et al. Neural mechanisms of transient neocortical beta rhythms: Converging evidence from humans, computational modeling, monkeys, and mice. Proc Natl Acad Sci U S A. 2016;113: E4885–94.

14. Khanna P, Carmena JM. Beta band oscillations in motor cortex reflect neural

population signals that delay movement onset. Elife. 2017;6. doi:10.7554/eLife.24573

15. Heinrichs-Graham E, Kurz MJ, Gehringer JE, Wilson TW. The functional role of post-movement beta oscillations in motor termination. Brain Struct Funct. 2017;222: 3075–3086.

16. Wessel JR. β-Bursts Reveal the Trial-to-Trial Dynamics of Movement Initiation and Cancellation. J Neurosci. 2020;40: 411–423.

17. Buzsáki G, Draguhn A. Neuronal oscillations in cortical networks. Science. 2004;304: 1926–1929.

18. van Wijk BCM, Beek PJ, Daffertshofer A. Differential modulations of ipsilateral and contralateral beta (de)synchronization during unimanual force production. Eur J Neurosci. 2012;36: 2088–2097.

19. McFarland DJ, Miner LA, Vaughan TM, Wolpaw JR. Mu and beta rhythm topographies during motor imagery and actual movements. Brain Topogr. 2000;12: 177–186.

20. Mary A, Wens V, Op de Beeck M, Leproult R, De Tiège X, Peigneux P. Age-related differences in practice-dependent resting-state functional connectivity related to motor sequence learning. Hum Brain Mapp. 2017;38: 923–937.

21. Sugata H, Yagi K, Yazawa S, Nagase Y, Tsuruta K, Ikeda T, et al. Role of beta-band resting-state functional connectivity as a predictor of motor learning ability. Neuroimage. 2020;210: 116562.

22. Ding Q, Lin T, Cai G, Ou Z, Yao S, Zhu H, et al. Individual differences in beta-band oscillations predict motor-inhibitory control. Front Neurosci. 2023;17: 1131862.

23. Chung JW, Ofori E, Misra G, Hess CW, Vaillancourt DE. Beta-band activity and connectivity in sensorimotor and parietal cortex are important for accurate motor performance. Neuroimage. 2017;144: 164–173.

24. Chettouf S, Rueda-Delgado LM, de Vries R, Ritter P, Daffertshofer A. Are unimanual movements bilateral? Neurosci Biobehav Rev. 2020;113: 39–50.

25. Ferbert A, Priori A, Rothwell JC, Day BL, Colebatch JG, Marsden CD. Interhemispheric inhibition of the human motor cortex. J Physiol. 1992;453: 525–546.

26. Duque J, Murase N, Celnik P, Hummel F, Harris-Love M, Mazzocchio R, et al. Intermanual Differences in movement-related interhemispheric inhibition. J Cogn Neurosci. 2007;19: 204–213.

27. Duque J, Mazzocchio R, Dambrosia J, Murase N, Olivier E, Cohen LG. Kinematically specific interhemispheric inhibition operating in the process of generation of a voluntary movement. Cereb Cortex. 2005;15: 588–593.

28. Giovannelli F, Borgheresi A, Balestrieri F, Zaccara G, Viggiano MP, Cincotta M, et al. Modulation of interhemispheric inhibition by volitional motor activity: an ipsilateral silent period study. J Physiol. 2009;587: 5393–5410.

29. Di Lazzaro V, Oliviero A, Profice P, Insola A, Mazzone P, Tonali P, et al. Direct demonstration of interhemispheric inhibition of the human motor cortex produced by transcranial magnetic stimulation. Exp Brain Res. 1999;124: 520–524.

30. Fleming MK, Newham DJ. Reliability of Transcallosal Inhibition in Healthy Adults. Front Hum Neurosci. 2016;10: 681.

31. Klein P-A, Duque J, Labruna L, Ivry RB. Comparison of the two cerebral hemispheres in inhibitory processes operative during movement preparation. Neuroimage. 2016;125: 220–232.

32. Perez MA, Cohen LG. Interhemispheric inhibition between primary motor cortices: what have we learned? J Physiol. 2009;587: 725–726.

33. Jung P, Ziemann U. Differences of the ipsilateral silent period in small hand muscles. Muscle Nerve. 2006;34: 431–436.

34. Kuo Y-L, Dubuc T, Boufadel DF, Fisher BE. Measuring ipsilateral silent period: Effects of muscle contraction levels and quantification methods. Brain Res. 2017;1674: 77–83.

35. Fling BW, Seidler RD. Task-dependent effects of interhemispheric inhibition on motor control. Behav Brain Res. 2012;226: 211–217.

36. Meyer BU, Röricht S, Gräfin von Einsiedel H, Kruggel F, Weindl A. Inhibitory and excitatory interhemispheric transfers between motor cortical areas in normal humans and patients with abnormalities of the corpus callosum. Brain. 1995;118 (Pt 2): 429–440.

37. Wassermann EM, Fuhr P, Cohen LG, Hallett M. Effects of transcranial magnetic stimulation on ipsilateral muscles. Neurology. 1991;41: 1795–1799.

38. Stefanou M-I, Desideri D, Belardinelli P, Zrenner C, Ziemann U. Phase Synchronicity of μ-Rhythm Determines Efficacy of Interhemispheric Communication Between Human Motor Cortices. J Neurosci. 2018;38: 10525–10534.

39. Vetter DE, Zrenner C, Belardinelli P, Mutanen TP, Kozák G, Marzetti L, et al. Targeting motor cortex high-excitability states defined by functional connectivity with real-time EEG-TMS. Neuroimage. 2023;284: 120427.

40. Hussain SJ, Cohen LG, Bönstrup M. Beta rhythm events predict corticospinal motor output. Sci Rep. 2019;9: 18305.

41. Torrecillos F, Falato E, Pogosyan A, West T, Di Lazzaro V, Brown P. Motor Cortex

Inputs at the Optimum Phase of Beta Cortical Oscillations Undergo More Rapid and Less Variable Corticospinal Propagation. J Neurosci. 2020;40: 369–381.

42. Illman M, Laaksonen K, Jousmäki V, Forss N, Piitulainen H. Reproducibility of Rolandic beta rhythm modulation in MEG and EEG. J Neurophysiol. 2022;127: 559–570.

43. Premoli I, Bergmann TO, Fecchio M, Rosanova M, Biondi A, Belardinelli P, et al. The impact of GABAergic drugs on TMS-induced brain oscillations in human motor cortex. Neuroimage. 2017;163: 1–12.

44. Fuggetta G, Fiaschi A, Manganotti P. Modulation of cortical oscillatory activities induced by varying single-pulse transcranial magnetic stimulation intensity over the left primary motor area: a combined EEG and TMS study. Neuroimage. 2005;27: 896–908.

45. Kawasaki M, Uno Y, Mori J, Kobata K, Kitajo K. Transcranial magnetic stimulation-induced global propagation of transient phase resetting associated with directional information flow. Front Hum Neurosci. 2014;8: 173.

46. Erickson B, Kim B, Sabes P, Rich R, Hatcher A, Fernandez-Nuñez G, et al. TMS-induced phase resets depend on TMS intensity and EEG phase. J Neural Eng. 2024. doi:10.1088/1741-2552/ad7f87

47. Stamoulis C, Oberman LM, Praeg E, Bashir S, Pascual-Leone A. Single pulse TMS-induced modulations of resting brain neurodynamics encoded in EEG phase. Brain Topogr. 2011;24: 105–113.

48. Canavier CC. Phase-resetting as a tool of information transmission. Curr Opin Neurobiol. 2015;31: 206–213.

49. Voloh B, Womelsdorf T. A Role of Phase-Resetting in Coordinating Large Scale Neural Networks During Attention and Goal-Directed Behavior. Front Syst Neurosci. 2016;10: 18.

50. Echeverria-Altuna I, Quinn AJ, Zokaei N, Woolrich MW, Nobre AC, van Ede F. Transient beta activity and cortico-muscular connectivity during sustained motor behaviour. Prog Neurobiol. 2022;214: 102281.

51. Bräcklein M, Barsakcioglu DY, Del Vecchio A, Ibáñez J, Farina D. Reading and Modulating Cortical β Bursts from Motor Unit Spiking Activity. J Neurosci. 2022;42: 3611–3621.

52. Bourguignon M, Piitulainen H, Smeds E, Zhou G, Jousmäki V, Hari R. MEG Insight into the Spectral Dynamics Underlying Steady Isometric Muscle Contraction. J Neurosci. 2017;37. doi:10.1523/JNEUROSCI.0447-17.2017

53. Mongold SJ, Piitulainen H, Legrand T, Vander Ghinst M, Naeije G, Jousmäki V, et al.

Temporally stable beta sensorimotor oscillations and corticomuscular coupling underlie force steadiness. Neuroimage. 2022;261: 119491.

54. Oldfield RC. The assessment and analysis of handedness: the Edinburgh inventory. Neuropsychologia. 1971;9: 97–113.

55. Rossini PM, Barker AT, Berardelli A, Caramia MD, Caruso G, Cracco RQ, et al. Non-invasive electrical and magnetic stimulation of the brain, spinal cord and roots: basic principles and procedures for routine clinical application. Report of an IFCN committee. Electroencephalogr Clin Neurophysiol. 1994;91: 79–92.

56. Tiffin J, Asher EJ. The Purdue pegboard; norms and studies of reliability and validity. J Appl Psychol. 1948;32: 234–247.

57. Oostenveld R, Fries P, Maris E, Schoffelen J-M. FieldTrip: Open source software for advanced analysis of MEG, EEG, and invasive electrophysiological data. Comput Intell Neurosci. 2011;2011: 156869.

58. Bigdely-Shamlo N, Mullen T, Kothe C, Su K-M, Robbins KA. The PREP pipeline: standardized preprocessing for large-scale EEG analysis. Front Neuroinform. 2015;9: 16.

59. Vigário R, Särelä J, Jousmäki V, Hämäläinen M, Oja E. Independent component approach to the analysis of EEG and MEG recordings. IEEE Trans Biomed Eng. 2000;47: 589–593.

60. Hupfeld KE, Swanson CW, Fling BW, Seidler RD. TMS-induced silent periods: A review of methods and call for consistency. J Neurosci Methods. 2020;346: 108950.

61. Garvey MA, Ziemann U, Becker DA, Barker CA, Bartko JJ. New graphical method to measure silent periods evoked by transcranial magnetic stimulation. Clin Neurophysiol. 2001;112: 1451–1460.

62. van den Wollenberg AL. Redundancy analysis an alternative for canonical correlation analysis. Psychometrika. 1977;42: 207–219.

63. Andersen RA, Cui H. Intention, action planning, and decision making in parietal-frontal circuits. Neuron. 2009;63: 568–583.

64. Halsband U, Ito N, Tanji J, Freund HJ. The role of premotor cortex and the supplementary motor area in the temporal control of movement in man. Brain. 1993;116 (Pt 1): 243–266.

65. Riemann BL, Lephart SM. The Sensorimotor System, Part II: The Role of Proprioception in Motor Control and Functional Joint Stability. J Athl Train. 2002;37: 80–84.

66. Ibáñez J, Del Vecchio A, Rothwell JC, Baker SN, Farina D. Only the Fastest

Corticospinal Fibers Contribute to β Corticomuscular Coherence. J Neurosci. 2021;41: 4867–4879.

67. Bonaiuto JJ, Little S, Neymotin SA, Jones SR, Barnes GR, Bestmann S. Laminar dynamics of high amplitude beta bursts in human motor cortex. Neuroimage. 2021;242: 118479.

68. West TO, Duchet B, Farmer SF, Friston KJ, Cagnan H. When do bursts matter in the primary motor cortex? Investigating changes in the intermittencies of beta rhythms associated with movement states. Prog Neurobiol. 2023;221: 102397.

69. Kuo Y-L, Kutch JJ, Fisher BE. Relationship between Interhemispheric Inhibition and Dexterous Hand Performance in Musicians and Non-musicians. Sci Rep. 2019;9: 11574.

70. Murase N, Duque J, Mazzocchio R, Cohen LG. Influence of interhemispheric interactions on motor function in chronic stroke. Ann Neurol. 2004;55: 400–409.

71. Iwama S, Yanagisawa T, Hirose R, Ushiba J. Beta rhythmicity in human motor cortex reflects neural population coupling that modulates subsequent finger coordination stability. Commun Biol. 2022;5: 1375.

72. Serrien DJ, Brown P. The functional role of interhemispheric synchronization in the control of bimanual timing tasks. Exp Brain Res. 2002;147: 268–272.

73. Morishita T, Timmermann JE, Schulz R, Hummel FC. Impact of interhemispheric inhibition on bimanual movement control in young and old. Exp Brain Res. 2022;240: 687–701.

74. Gu B, Wang K, Chen L, He J, Zhang D, Xu M, et al. Study of the Correlation between the Motor Ability of the Individual Upper Limbs and Motor Imagery Induced Neural Activities. Neuroscience. 2023;530: 56–65.

75. Engel AK, Fries P. Beta-band oscillations--signalling the status quo? Curr Opin Neurobiol. 2010;20: 156–165.

Declarations

Funding. Christian Georgiev was supported by an Aspirant Research Fellowship awarded by the Fonds de la Recherche Scientifique (F.R.S.-FNRS; Brussels, Belgium; grant 1.A.211.24F). Scott Mongold was supported by an Aspirant Research Fellowship awarded by the F.R.S.-FNRS (Brussels, Belgium; grant FC 46249). Pierre Cabaraux was supported by a Clinical Researcher Fellowship awarded by the F.R.S.-FNRS (Brussels, Belgium; grant 40024164). Gilles Naeije is postdoctorate Clinical Master Specialist at the FRS-FNRS (Brussels, Belgium). The project was supported by grants of the Fonds de la Recherche Scientifique (F.R.S.-FNRS, Brussels, Belgium; grant MIS F.4504.21), and of the Brussels-Wallonia Federation (Collective Research Initiatives grant) awarded to Mathieu Bourguignon. This publication was supported by the Walloon Region as part of the FRFS-WELBIO strategic axis.

***CRediT Author contribution*: Christian Georgiev**: Conceptualization, Investigation, Formal analysis, Visualization, Writing – original draft. **Scott J. Mongold**: Conceptualization, Investigation, Writing – review & editing. **Pierre Cabaraux**: Investigation, Writing – review & editing. **Gilles Naeije**: Writing – review & editing. **Julie Duqué:** Writing – review & editing. **Mathieu Bourguignon**: Conceptualization, Formal analysis, Visualization, Data curation, Supervision, Writing - review & editing.

Declaration of competing interest. The authors have no relevant financial or non-financial conflicts of interests to disclose.

Supplementary Results 1

Participants' scores on the PPT ranged between 11 and 19 (Mean = 15, SD = 2) for the Left Hand subset, between 10 and 22 (Mean = 16, SD = 2) for the Right Hand subset, between 7 and 16 (Mean = 12, SD = 2) for the Both Hands subset, and between 22 and 51 (Mean = 37, SD = 7) for the Assembly subset. These results are consistent with the findings of other investigators and with PPT population norms from healthy adults [74,76].

Two-tailed Spearman correlation analyses revealed that, as expected, the contrasts of ipsilateral/contralateral beta suppression ($\Delta\beta_{size}$ and $\Delta\beta_{depth}$) were correlated with each other (r = 0.45, p = 0.004). Likewise, the measures of iSP (latency, duration, and normalized area) were also correlated with each other ($0.46 \leq |r| \leq 0.73$, all $p < 0.05$) in the respective expected direction. However, no correlation between the $\Delta\beta_{size}$ and $\Delta\beta_{depth}$ and measures of the iSP was found ($0.26 \leq p \leq 0.57$) and, with the exception of a moderate correlation between the $\Delta\beta_{size}$ and the $PPTc_1$ (r = 0.37, p = 0.018) no measures of beta rhythm or of iSP correlated with any measure of bimanual motor performance (Figure S1).

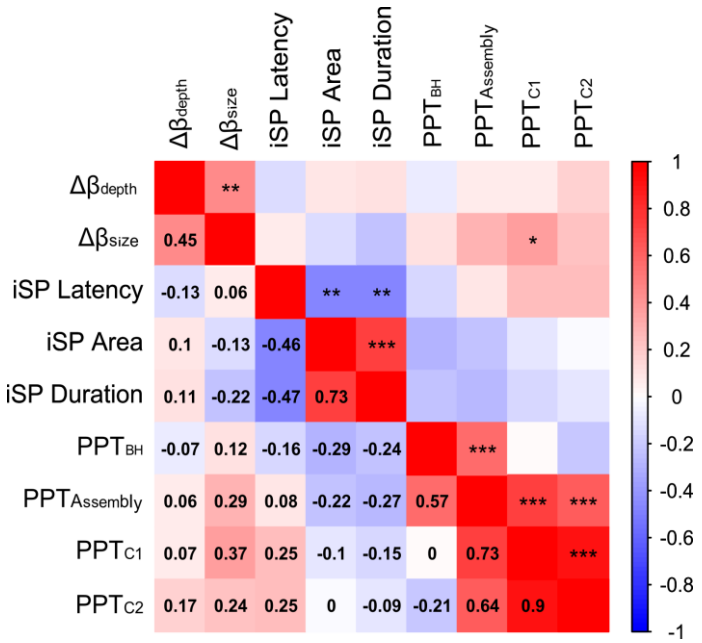

*Figure S1. Pairwise correlations between the measures of beta, the iSP, and the behavioral tests. Values below the main diagonal depict rho values, while values above the main diagonal depict the corresponding significance levels with: *, $p < 0.05$; **, $p < 0.001$; ***, $p < 0.0001$.*

References

74. Gu B, Wang K, Chen L, He J, Zhang D, Xu M, et al. Study of the Correlation between the Motor Ability of the Individual Upper Limbs and Motor Imagery Induced Neural Activities. Neuroscience. 2023;530: 56–65.

76. Yeudall LT, Fromm D, Reddon JR, Stefanyk WO. Normative data stratified by age and sex for 12 neuropsychological tests. J Clin Psychol. 1986;42: 918–946.